

Cavitation-Mediated Transcutaneous Delivery of Protein and Nucleotide-based Antigen for Rapid High-level Immune Responses

Johanna K Hettinga, Brian Lyons, Joel Balkaran, Pramila Rijal, Darcy Dunn-Lawless, Lisa Caproni, Michael Gray, Kenneth S. Suslick, Constantin C Coussios, and Robert C Carlisle*

Alternatives are needed to remove the pain, injury, cross-infection, and hazardous waste associated with needle and syringe (N+S)-based vaccination. Reported here is the use of novel ultrasound-responsive protein cavitation nuclei (pCaN), formed using the model antigen bovine serum albumin (BSA), to achieve effective transcutaneous delivery. Upon exposure to ultrasound (US), these pCaN instigate cavitation events which propel themselves and co-located DNA vectors into the skin. US parameters as well as pCaN and DNA concentration are refined to achieve optimal expression of encoded luciferase transgene. Twenty-four hours post-treatment, luciferase expression in the skin, by IVIS imaging, was $1.67 \times 10^6 \pm 941943$ photons per sec for N+S intradermal injection and $1.49 \times 10^6 \pm 261832$ for cavitation-mediated delivery ($p > 0.05$). Hence, there is no significant difference in luciferase level achieved, but improved homogeneity and reproducibility of expression are evident in mice treated using US-mediated cavitation. Despite this equivalence in luciferase levels, a $>5\times$ higher level ($p < 0.02$) of anti-luciferase antibodies is achieved when cavitation is used versus N+S injection. Antibody levels against BSA, resulting from the use of BSA pCaN, are equivalent for the two groups. PCaN can be formed from a range of antigenic proteins and DNA can encode a range of antigenic proteins, so this approach has wide-ranging implications for needle-free vaccination.

1. Introduction


Over the last 200 years, strategies for achieving protective immunity against pathogenic disease have developed to the stage where vaccination represents one of humankind's most important and impactful endeavors.^[1] However, whilst a range of increasingly sophisticated vaccine vectors is now available, the methods of administering vaccines have changed a little over the last century. Hypodermic needle and syringe (N+S) delivery has maintained its prominence despite serious issues with pain, cross-infection, injuries, and the generation of hazardous waste. Indeed, figures from a 2004 analysis showed that 30 million needle stick injuries resulted from the 800 million prophylactic inoculations administered that year.^[2,3] Although safety improvements have been successfully implemented,^[4] the substantial pain, distress, and potential for cross-infection with blood-borne pathogens, remains.^[5] In response to this worrying iatrogenicity, researchers have looked to develop alternative

J. K Hettinga, B. Lyons, J. Balkaran, D. Dunn-Lawless, M. Gray,
C. C Coussios, R. C Carlisle
BUBBL group
Institute of Biomedical Engineering
Department of Engineering Science
University of Oxford
Oxford OX3 7LD, UK
E-mail: robert.carlisle@eng.ox.ac.uk

P. Rijal
Centre for Translational Immunology
Chinese Academy of Medical Sciences Oxford Institute
University of Oxford
Oxford OX3 7BN, UK

L. Caproni
Touchlight Ltd
Morelands & Riverdale Buildings
Lower Sunbury Road, Hampton TW12 2ER, UK

K. S. Suslick
Department of Chemistry
University of Illinois
Urbana, IL 61801, USA

 The ORCID identification number(s) for the author(s) of this article can be found under <https://doi.org/10.1002/adtp.202300102>

© 2023 The Authors. *Advanced Therapeutics* published by Wiley-VCH GmbH. This is an open access article under the terms of the Creative Commons Attribution License, which permits use, distribution and reproduction in any medium, provided the original work is properly cited.

DOI: 10.1002/adtp.202300102

approaches that might allow vaccination without the use of a needle. A range of technologies have been investigated including microneedles, jet/ballistic devices, electroporation, and chemical peels.^[6–9]

Exposure of a gas bubble in solution to the alternating rarefactional and compressional cycles of an ultrasound (US) wave can lead to the expansion and collapse of the bubble, creating microstreaming and shockwaves. Such perturbation can then propel therapeutic agents within the solution over distances of 100s of microns and enable their delivery through biological barriers.^[10] We have previously demonstrated that an inert gas-stabilizing polymeric cup formulation can nucleate sustained inertial cavitation and thereby assist in the delivery of antibodies and viruses into and throughout solid tumors.^[11] Crucially, the sustained inertial cavitation, which can be maintained over several cycles of ultrasound (US) exposure using solid gas stabilizing particles, is key to optimizing such delivery.^[12] Building on these mechanistic findings we have also extended the approach to the delivery of drugs and protein vaccines into and through the skin. We have demonstrated both significant increases in the penetration and transcutaneous delivery of model antigen ovalbumin in mice.^[13] Such studies have helped us establish US parameters (frequency, pressure range, duty cycle) that could be both safe and effective.

If delivery into the dermal layers is to be used for small molecule and protein-based drugs, it would be necessary, but also extremely challenging, to match the dose loading achieved by N+S. However, the delivery of nucleotide-based vectors for vaccination removes this requirement, making the approach less challenging and more feasible. This is because the levels of amplification provided by the transcription and translation of nucleotide into protein and in the instigation of an immune response against such protein may negate the loss in actual initial delivery efficiency compared to N+S. Furthermore, whilst N+S is often reliant on delivery to the intramuscular compartment, dermal delivery provides access to a richer immune milieu, which may allow a lower dose to achieve a more marked immune response than would be achieved with a high dose delivered into the muscle.^[14] Kenney et al have demonstrated this general concept for influenza vaccination, where one-fifth of a full dose of vaccine administered ID can match the level achieved by injecting into the muscle.^[15]

DNA or RNA-based vaccines provide notable advantages in terms of the ease, speed, and cost of production and storage compared to alternatives.^[16] Whilst RNA vaccines have made an enormous impact, issues relating to stability and their need to be formulated into lipid nanoparticles mean exploring and optimizing the utility of DNA remains a worthy pursuit. Especially as DNA can now be produced using the multi-gram enzymatic cell-free “doggybone” DNA platform (dbDNA, Touchlight Ltd).^[17] This improved production and greater stability^[18] mean that provided issues with inefficient delivery into cell nuclei can be overcome, DNA is well suited for use in vaccination against prevalent and rapidly changing pathogens such as influenza and coronaviruses. However, whilst the rationale for the use of naked DNA in vaccination is strong, its translation into clinical practice has been stymied by the dearth of technologies that can provide pain-free, reliable, measurable, and effective delivery of DNA. Technologies such as electroporation and microneedles^[19,20] and re-

cently a combination of these two,^[21] have made good progress, with promising clinical trial data for electroporation-mediated delivery of the SARS-CoV-2 vaccine.^[22] However, to date, there has yet to be a DNA vaccine with FDA approval for human use, and limitations of these approaches relating to pain, skin irritation, achievable dosage levels, required dosing durations, and the lack of feedback on the success of dosing, remain. There is therefore value in considering alternative delivery approaches. Cavitation is an interesting prospect in this context, as it can provide a convective stimulus for the movement of large molecules, it can be applied without pain or damage, and passive cavitation detection can provide real-time feedback on the success of the delivery process.^[23] Furthermore, there is evidence to suggest that US exposure alone results in direct activation of immune cells within the skin, as evidenced by Tezel et al who demonstrated 20 kHz US exposure alone led to activation of Langerhans cells.^[24] Such work raises the prospect that if utilized appropriately US-based delivery can even help increase the level of the resulting anti-antigen immune response.

Here we report the combination of US technology with DNA vectors to demonstrate that cavitation-mediated delivery can achieve delivery, which although far less effective in terms of dose transferred, can match transgene expression levels and immune outputs achieved using conventional N+S delivery. This is achieved with US parameters similar to those we have previously shown to be effective and safe.^[13] It is notable that the inclusion of pre-formed cavitation nuclei reduces the pressure amplitude required to instigate cavitation and so reduces the power requirements of the system used, as well as reducing the potential for temperature rises which may otherwise lead to damage of the therapeutic cargo and/or the skin. It is also noteworthy that our previous studies have relied on the use of inert synthetic polymeric ‘nanocups’, which are effective cavitation nuclei but have no intrinsic capacity to enhance immune response.^[13] Hence, in the work presented here the use of novel “active” protein-based cavitation nuclei (pCaN), rather than inert polymeric nanocups or microbubbles, means that the cavitation agent is not only responsible for the delivery of the DNA but may also ultimately be selected with enhancement of the immune response in mind. Experiments using DNA encoding the luciferase reporter gene demonstrated that US-mediated cavitation could provide a level and area of delivery with more favorable reproducibility than intradermal N+S delivery. Crucially, the capability we demonstrate to monitor cavitation during delivery helps establish relationships between the level of cavitation and the level of delivery achieved. We demonstrate that a successful immune response can be generated against pCaN comprised of the model protein bovine serum albumin (BSA) and against the model luciferase product of the luciferase encoding DNA vector delivered. We then demonstrate delivery of DNA encoding the H1N1/Cal09 influenza antigen by cavitation can instigate a substantial antibody and cellular response. These findings raise the prospect that a range of DNA vectors encoding a range of targets from pathogenic antigens can be delivered by pCaN constructed out of immune-modulatory proteins designed to amplify the response. Such an adaptable and rapidly deployable platform approach has potentially powerful utility in the treatment of rapidly emerging and evolving pathogens.

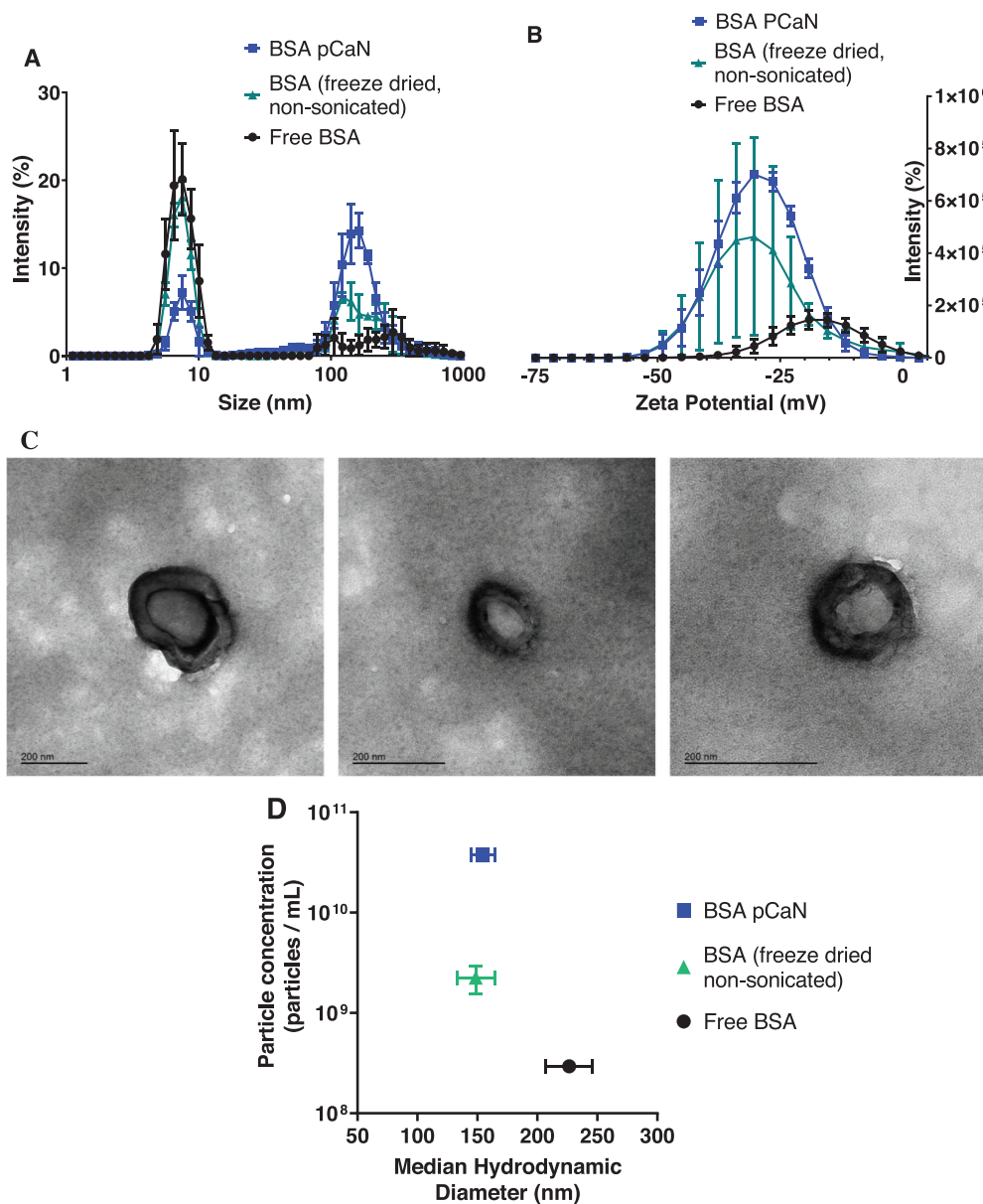


Figure 1. Formulation and characterization of protein cavitation nuclei (pCaN) made from BSA. In panel A) a dynamic light scattering profile of free bovine serum albumin (BSA) is shown in black circles, and the profile for pCaN particles made using BSA is shown in blue squares. Control sample whereby BSA protein was freeze-dried without first being sonicated is shown as green triangles. Panel B) shows zeta potential analysis comparing the same 3 formulations as in A). Data is typical of 3 repeat formulations, error bars represent standard deviations of $n = 3$ values. Panel C) shows a selection of electron microscopy images of BSA pCaN (free BSA and non-sonicated freeze-dried BSA failed to produce imageable particles). Panel D) shows a Videodrop analysis of BSA pCaN, freeze-dried non-sonicated BSA protein, or free BSA ($n = 3$), error bars show standard deviation. All analysis methods are described in the Experimental Section.

2. Results and Discussion

2.1. Physicochemical Characterization of Protein Cavitation Nuclei (pCaN)

Soninating mixtures of protein (BSA) and volatile solvent (Hexane) followed by removal of the volatile solvent under vacuum (see Experimental Section) created nanoscale protein particles capable of entrapping air (pCaN). DLS analysis, (see Experimental

Section) (Figure 1A) demonstrated that control non-formulated BSA (black circles) produced a dominant peak at 5–10 nm representing non-modified BSA and a peak at 20–100 nm understood to be BSA aggregates. Control BSA samples which were freeze-dried but not probe-sonicated (green triangles) produced a similar profile. In contrast, the pCaN sample (blue squares), which underwent probe sonication and freeze drying, had a predominant peak with an average diameter ≈ 200 nm. Notably, a peak of non-formulated BSA (5-10 nm) was still evident in this

sample but was much reduced in size compared to the control non-formulated BSA sample and the non-probe sonicated control sample. Zeta potential (see Experimental Section) demonstrated the pCaN particles to have a surface charge of between -20 and -30 mV, in accordance with their low propensity to aggregate (Figure 1B). Images acquired by transmission electron microscopy (see Experimental Section) demonstrated a size range in accordance with the DLS data and the presence of indented sub-micron protein particles with morphologies suggestive of an ability to entrap gas bubbles (1C). Videodrop data further verified the size range and demonstrated a 10-fold increase in particle concentration with pCaN formulation (5×10^{10} mL⁻¹) compared to controls made by freeze-drying protein without first sonicating it (5×10^9 mL⁻¹).

2.2. In vitro Ultrasound Response of pCaN

The ability of pCaN to act as nuclei for cavitation was tested using the set-up outlined in the schematic in Figure S1B (Supporting Information). The pCaN sample was loaded into the exposure chamber and exposed to a pressure ramp running up to 2.1 MPa (peak negative). Acoustic exposure parameters were as described in Figure S1D (Supporting Information) and acoustic emissions were detected and processed as described in Experimental Section. It is evident from the time versus frequency versus energy spectral density plot (Figure S2, Supporting Information) that pCaN can nucleate cavitation for sustained periods at such pressure amplitudes. The wide range of frequencies detected by the passive cavitation detector indicated that substantial amounts of inertial cavitation were generated. Notably, there was no relatively substantial and sustained cavitation detected when the sample holder contained water, unmodified BSA, or BSA which had been freeze-dried but not probe-sonicated (Figure S2D,C,B, Supporting Information). The ability to generate over a minute of broadband “inertial” cavitation has previously been associated with in vivo utility and superior performance compared to short-lived harmonic-dominated narrowband acoustic emissions associated with microbubble formulations.^[12,13]

2.3. In Vivo Delivery of Luciferase Encoding DNA using pCaN to Nucleate Ultrasound Mediated Cavitation

Whilst in vitro analysis had demonstrated pCaN to be capable of nucleating a robust and substantial level of cavitation activity, to identify optimal parameters for in vivo DNA delivery, a range of experimental conditions had to be explored. This was achieved using BALB/c mice prepared and treated as described in the Experimental Section, a luciferase encoding DNA plasmid (Experimental Section), and the US set-up and parameters as shown in the schematic in Figure S1 (Supporting Information). Figure 2A demonstrates the impact of amplitude of exposure pressure on the cavitation frequency spectrum and level of energy detected from the focal region, which encompasses the sample-skin interface.

Notably, the type of pCaN-nucleated cavitation activity observed in vivo was in accordance with that observed in vitro, characterized by consistent and sustained broadband acoustic emissions which lasted the full 5 min of exposure at pressures of

1.5 MPa and above. During in vivo studies, a low level of cavitation was also detected and recorded in the absence of pCaN (Figure S3A in Supporting Information 0% pCaN panel), most probably the result of air entrapment on the mouse skin, but this level was more than two orders of magnitude lower than in the presence of pCaN.

For quantification of the expression of the luciferase transgene, IVIS imaging (see Experimental Section) was performed 24 h after cavitation-mediated delivery at the range of peak negative pressures from 0.4 MPa to 2.0 MPa, Figure 2B–D. Notably, negligible expression was evidenced in the presence of US but the absence of pCaN, in agreement with the low cavitation levels detected (Figure S3B, Supporting Information). In contrast, substantial areas of successfully transfected skin were evidenced within the exposure region when pCaN was used. Indeed, a relationship was observed between the pressure applied and the luciferase expression that resulted. Specifically, as the exposure pressure and cavitation energy, (calculated via a summation metric, denoted Total Acoustic Sensor Energy (TASE) in μ J as described in the Experimental Section), increased, the level of luciferase expression increased until a plateau at $\approx 1 \times 10^6$ photons per second was reached using 1.5 or 1.7 MPa (equivalent to 10–20 μ J TASE). A decline in luciferase expression was evident in the group of mice exposed to 2.0 MPa (Figure 2C,D). Although by 24 h there was no overt sign of skin damage in any mouse when studied 10 min after completion of the 5 min exposure, redness was evident in mice treated at 2.0 MPa, such reddening may indicate damage to target cells and explain the relatively lower luciferase activity after 24 h compared to treating at 1.7 MPa.

As 1.7 MPa provided the best balance of reproducible activity with minimal skin reddening at 10 min, it was chosen for further experiments to optimize exposure duration (Figure 3). The ability of the pCaN to produce sustained broadband-frequency-rich cavitation signals was shown by the linear relationship between exposure duration and measured TASE cavitation energy, which could persist for at least 600 seconds (Figure 3A). Notably, the optimal length of exposure proved to be 120 seconds, and when 300 or 600 s exposure durations were used a relative decrease in IVIS signal was detected at 24 h post-exposure (442 750 vs 331 000 or 283 250 photons per second mean values) (Figure 3B). This experiment also helped further profile the relationship between TASE and luciferase expression (Figure 3C), with levels of between 10 and 20 TASE proving optimal. Visual assessment of skin at 10 min after completion of exposure demonstrated that the transient reddening of the skin was predictive of areas that would show decreased luciferase signal at 24 h (Figure 3D). The strong relationship between cavitation level measured at the time of treatment and the level of transgene expression achieved 24 h later, adds powerful potential clinical utility to this approach and provides a differentiator to other non-N+S approaches which currently provide no such feedback on the success or failure of dosing. It also provides an insight into the mechanisms underpinning the delivery observed. The impact of particle displacement and shear stress on the stratum corneum and cell membranes within the dermis, which results from the microstreaming and micro-jetting caused by stable and inertial cavitation, has been strongly implicated in sonophoresis and sonoporation and seems to be required here.^[25,26]

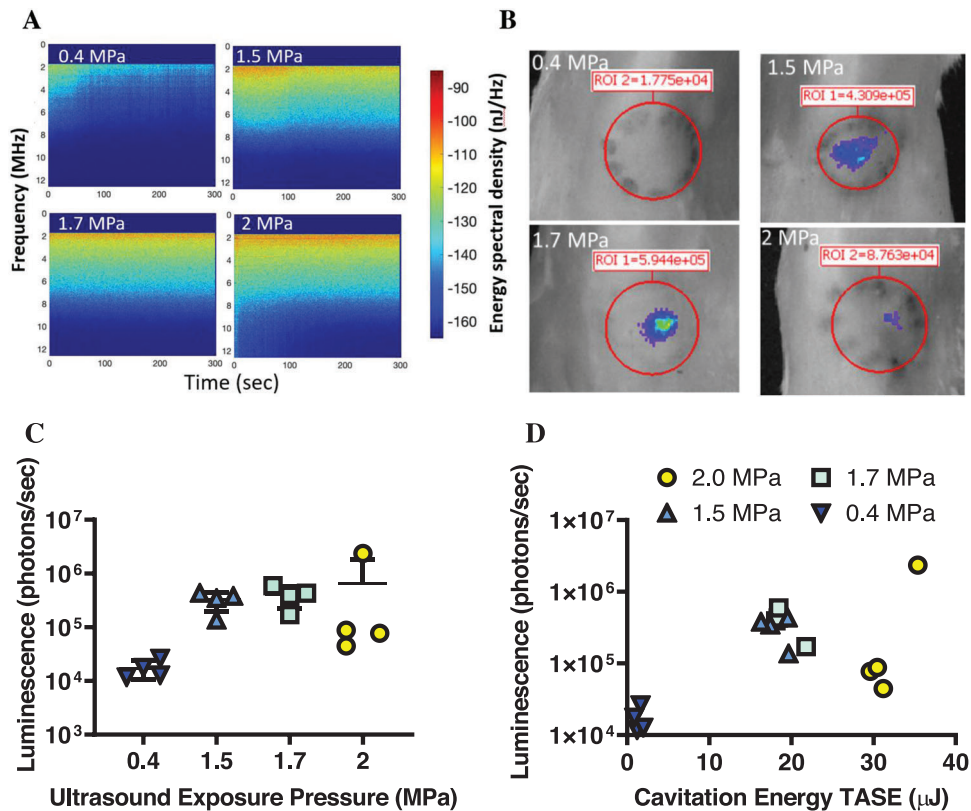


Figure 2. Influence of US exposure pressure on the level and duration of cavitation nucleated by BSA pCaN and its impact on reporter gene expression in the skin. The frequency and energy spectral density of acoustic emissions as a function of time are shown for pCaN exposed to 0.4, 1.5, 1.7, or 2.0 MPa (peak negative) US at 0.265 MHz for up to 5 min (panel A). The luciferase expression resulting from the cavitation-mediated transfer of luciferase encoding plasmid DNA into mouse skin at these 4 pressures, as measured by IVIS at 24 h post-treatment (see Experimental Section) is in panel B. The quantified luciferase expression from the 4 pressures at 24 h, is shown in panel C, 4 data points with means shown by horizontal lines and error bars showing standard deviation values. The relationship between the summed cavitation energy (μ Joules as calculated in the Experimental Section) at the time of exposure and the level of luciferase expression detected at 24 h is shown in panel D. The US and mouse set-up as shown in Figure S1 (Supporting Information) was used.

2.4. Comparison of pCaN Nucleated Cavitation to Intradermal N+S for Delivery of DNA

US-mediated cavitation is unlikely to match the ability of N+S to move total DNA dose into the dermal compartment. However, there is a possibility that the target immune-cell-rich milieu in the dermal compartment can be accessed and activated in a more effective, controlled, and reproducible way using this US technology than by N+S. It is also notable that the membrane-disrupting activity of cavitation^[27] may provide a mechanism for passage through both the cell and nuclear membranes, a mechanism not offered by N+S. Hence, a direct comparison of mice exposed to 90 μ g of DNA by optimized cavitation-mediated delivery or dosed with 90 μ g of DNA by intradermal injection, was performed and luciferase expression was measured 24 h later by IVIS (Figure 4A). Notably, no significant difference ($p > 0.05$) was evident between the expression levels achieved using the two approaches, but the cavitation group showed considerably improved reproducibility between mice and better uniformity to the area over which expression was observed. The question of how much DNA was actually delivered into the skin to achieve these levels of expression was addressed by the rescue of the skin and

quantitative PCR (Experimental Section). Figure 4B shows the quantified initial DNA delivery (see '0' h) and DNA retention after 24 h (see '24' h) for I.D. injection or cavitation-mediated delivery. Notably, only $\approx 0.13\%$ of the DNA in the sample holder entered the skin during the exposure to US, compared to over 96% with N+S delivery. However, when considered with respect to the level of transgene expression evident 24 h later (Figure 4A) the benefit of cavitation-mediated delivery becomes apparent. Specifically, when the luciferase flux at 24 h was calculated per DNA copy actually delivered (Figure S4, Supporting Information), on average 30-fold more DNA was needed per flux produced following I.D. injection compared to cavitation-mediated delivery. This indicates a far greater activity of DNA delivered transcutaneously via cavitation compared to I.D. injection.

A further notable observation was that the process of DNA clearance from the injection site appeared far more effective following I.D. injection than cavitation-mediated delivery. Indeed, by the 24 h time point, a 340-fold decrease in the mean level of DNA was observed following I.D. injection, compared to just a 5.6-fold non-significant ($p > 0.05$) decrease following cavitation-mediated delivery (Figure 4B). This emphasizes the dose wastage that can take place within the body following N+S injection.

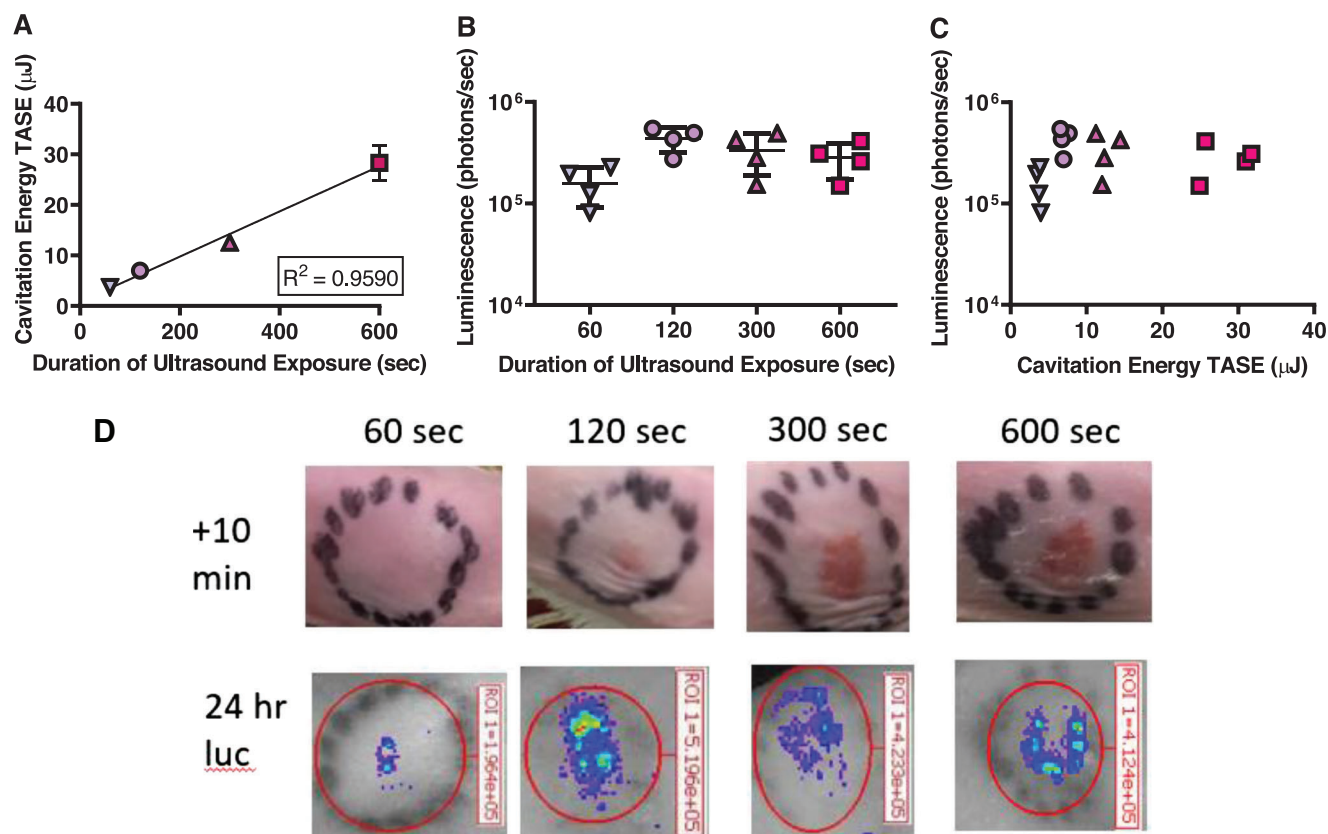


Figure 3. Influence of US exposure time on the level and duration of cavitation nucleated by BSA pCaN and the level of DNA reporter gene expression and skin damage. The sum cavitation energy detected as a result of exposure of pCaN to 1.7 MPa, 0.265 MHz US for 60, 120, 300, or 600 s is shown in panel A. The impact of duration of exposure on the level of luciferase expression from delivery of luciferase encoding plasmid DNA into the skin is shown in panel B, $n = 4$ horizontal lines represent the mean values, and error bars show the standard deviations. Panel C shows the relationship between the sum energy detected in μ Joules (calculated as described in the Experimental Section) during the time of exposure and the level of luciferase expression detected 24 h later. Panel D details the reddening of skin within the exposed area directly after treatment and its impact on luciferase expression from the delivered DNA plasmid at 24 h.

Previous work to profile DNA pharmacokinetics and biodistribution following I.D. injection has identified high variability of injection site retention,^[28] distribution to a wide range of organs^[29] and a low proportion of keratinocytes which achieve expression upon being exposed to DNA,^[30] but to our knowledge, ours is the first study to quantify the % of DNA injected that is retained at the injection site. Notably, in accordance with previous studies,^[13] no evidence of marked change to the composition or structure of the skin was observed following cavitation exposure using these parameters or I.D. injection (Figure 4C). Restriction of exposures to 1.7 MPa and 2 min, prevents skin damage and induces no increase in temperature at 1.7 MPa (see Figure S8, Supporting Information). Previous studies have shown cavitation does not impact the structure or function of small molecule, protein, or nucleotide-based therapeutics.^[31]

Having established that equivalence of transgene expression could be achieved, it was next important to probe how such expression converted into immune responses against the expressed protein. To achieve this, mice were primed with DNA expressing luciferase delivered via transcutaneous US-mediated delivery using BSA pCaN, or using an I.D. injection of luciferase DNA and BSA (at levels matched to those in the sample holder of the cav-

itation group). Three weeks later a homologous boost was performed. IVIS imaging was performed 24 h after each dosing which verified the success of the delivery and showed that I.D. injection and cavitation-mediated delivery achieved mean levels of expression that were not significantly different ($p > 0.05$) (data not shown). Analysis of anti-luciferase antibody levels (by ELISA, see Experimental Section) at day 42 post-prime demonstrated a substantial (>10-fold) and significant ($p < 0.02$) increase in the concentration of anti-luciferase antibodies present in the US group compared to the I.D. group (Figure 5A), as ascertained with reference to a standard curve established with known concentrations of a commercial standard anti-luciferase antibody. When these serum samples were titrated out, a 6400-fold dilution of serum from cavitation-treated mice matched the absorbance values achieved with a 1600-fold dilution of serum for I.D. injected mice (Figure 5B). It is notable that the 5 to 10-fold enhancement of antibody response achieved in the US-mediated cavitation group (Figure 5) was generated from the initial delivery of 700-fold less DNA compared to I.D. injection and equivalent level of luciferase expression (Figure 4).

We have demonstrated previously that cavitation nuclei can self-propel into the skin as they nucleate cavitation.^[13] As the

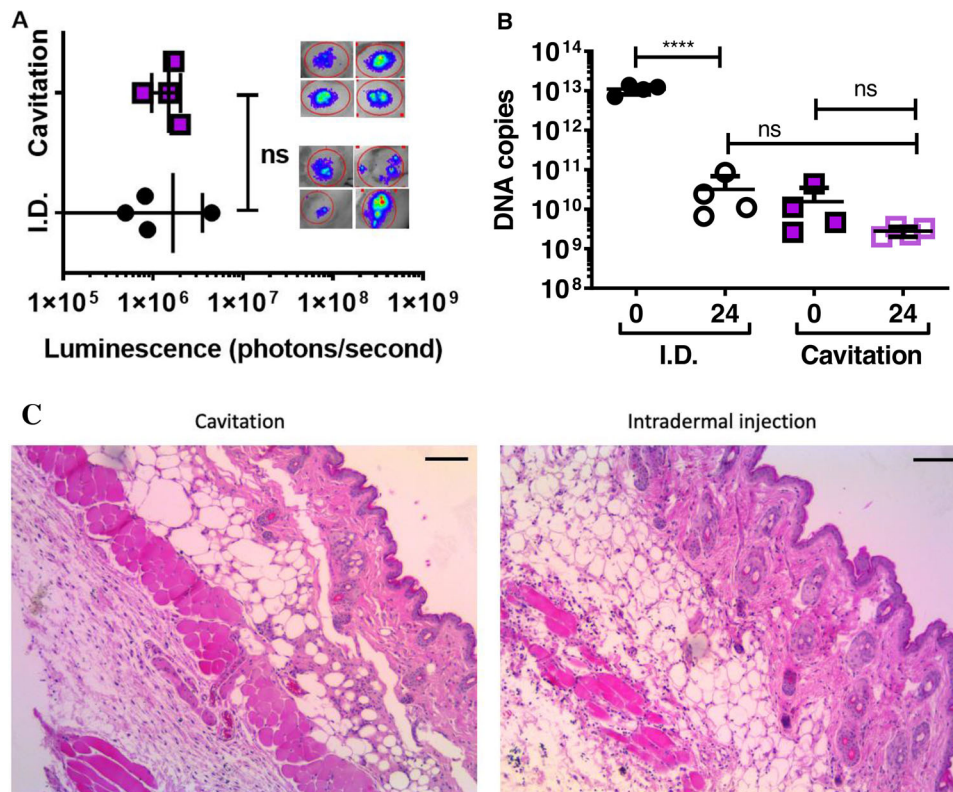


Figure 4. Delivery of DNA luciferase plasmid into the skin using US-mediated pCaN-nucleated cavitation compared to intradermal N+S delivery. The level of luciferase expression from delivery of luciferase encoding plasmid DNA into the skin is shown in panel A, $n = 4$ lines represent the mean values, error bars show the standard deviations, purple squares represent cavitation mediated delivery, black circles show delivery via intradermal N+S ('I.D.'). Inset pictures represent the images of the 4 US exposed or injected regions of skin for each treatment group at 24 h. Panel B shows the QPCR quantification of DNA delivered into the skin directly ('0') after the 2 min exposure at 1.7 MPa, 0.265 MHz or after intradermal injection and the level of DNA present at 24 h post-delivery ('24'). $N = 4$, mean shown with error bars representing standard deviation. ns = $p > 0.05$, **** = $p < 0.0001$. 4C shows representative skin sections taken from cavitation or I.D. treated mice at 24 h and stained with haematoxylin and eosin, (as described in Experimental Section). Scalebar represents 100 μm .

pCaN can be manufactured from immunogenic protein this system therefore offers two different immunisation options: the protein encoded by the delivered DNA and the protein used to formulate the pCaN which is then used to deliver the DNA. Hence, the level of response against BSA pCaN used in the US delivery group was compared to I.D. injection of BSA pCaN (equivalent amount to that in the sample holder of the cavitation group). Rescue of skin directly (i.e. '0' h) after US exposure and ELISA for the amount of BSA pCaN delivered (see Experimental Section), showed just 1.6% of the BSA dose was delivered by cavitation compared to $\sim 100\%$ dose delivery for I.D. injection (Figure 5C). By 24 h a ≈ 50 -fold reduction in the BSA recovered from I.D. injected skin was observed whereas no detectable BSA was present in the cavitation delivery group. Despite this differential, the anti-BSA antibody response achieved in both groups showed no statistically significant difference ($p > 0.5$) (Figure 5D) at any time point, with levels rising from day 7 to reach a plateau at day 42.

Whilst luciferase responses offer a means of linking delivery level (by QPCR), to expression (by IVIS imaging) to immune response (by anti-luc ELISA) it is important to validate if this approach has utility with a therapeutically relevant antigen. "To achieve this a plasmid construct expressing the influenza haemagglutinin (HA) protein Cal09" in combination

with a perforin-encoding adjuvant plasmid was delivered using I.D. injection or BSA pCaN nucleated cavitation. The dosing schedule matched that used for anti-luciferase response studies in Figure 5 and in addition to serum samples being collected for antibody profiling, spleen samples were taken at cull for ELISpot analysis of cellular responses.

Figure 6A,B shows that in contrast to the anti-luciferase antibody response, the level of anti-Cal09 HA antibodies was higher following I.D. injection than following cavitation-mediated delivery. Notably, when the affinity of the antibodies present was tested (see Experimental Section) the serum from cavitation-treated mice matched that from I.D. injected mice (Figure 6C). ELISpot analysis (see Experimental Section) (Figure 6D) showed the presence of Cal-09 HA reactive splenocytes in cavitation-treated mice and in I.D. injected mice, with no significant difference in the levels ($p > 0.05$) between the two groups, but a higher trend in the I.D. injected group.

3. Discussion and Conclusion

The work reported here describes a needle-free means for achieving delivery of DNA vectors into the dermal compartment. Previous studies have demonstrated the attractiveness of the

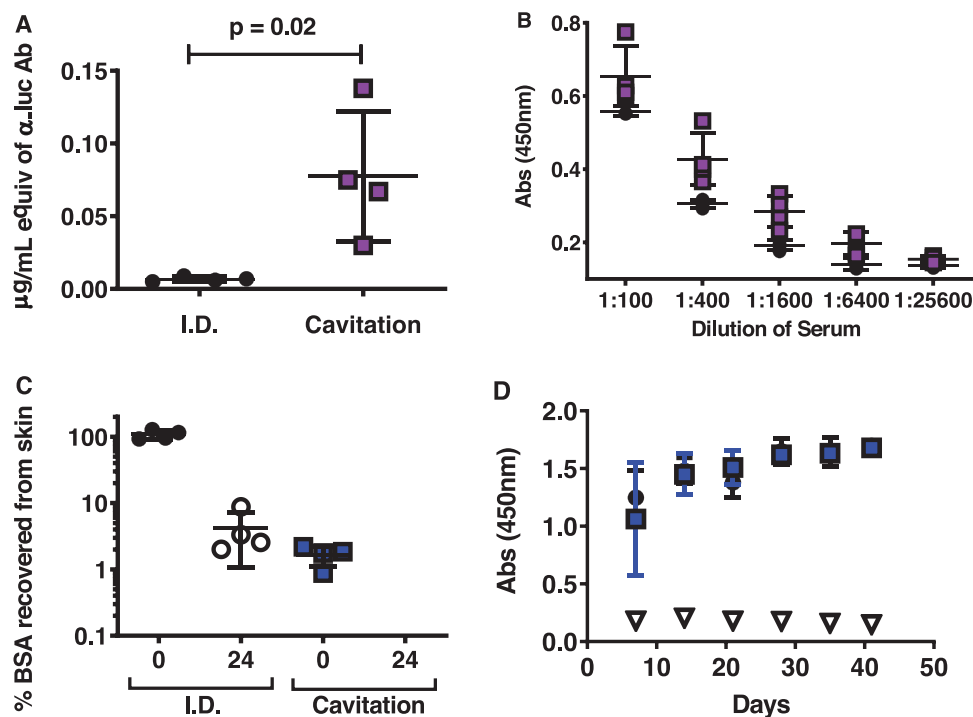


Figure 5. Antibody responses to BSA pCaN and luciferase protein following cavitation-mediated BSA pCaN nucleated delivery or intradermal injection with N+S. Panel A shows the antibody response raised by day 42 against luciferase protein as a result of priming and boosting with I.D. injected, or cavitation delivered, luciferase-expressing plasmid. Concentration in serum was calculated using a standard curve of known concentration of anti-luciferase antibody (see Experimental Section). Panel B shows the titer profile of the anti-luciferase antibodies raised. Panel C shows the amount of BSA delivered by I.D. injection of BSA pCaN or by cavitation nucleated by BSA pCaN directly after dosing as well as showing the dose still present 24 h later. Panel D shows the antibody response to BSA as assessed by ELISA, black circles = I.D., purple square = cavitation, triangles = untreated control. In all panels $n = 4$, standard deviations shown, a two-tailed unpaired student t-test used for data with 2 groups, ANOVA where >2 groups, and the significance level stated on the graphs.

dermal compartment as a vaccination target,^[15] and how the application of US can stimulate the immune system. In the *in vitro* setting Giantulli et al demonstrated IL6 release from human keratinocytes upon exposure to 1 MHz US, whilst *in vivo* Tezel et al demonstrated the activation of Langerhans cells in mouse skin upon exposure to 20 kHz US^[24,32] Whilst such findings show potentially detrimental or beneficial effects depending on the specific application they also demonstrate that there is a wide US parameter space to explore and refine to achieve any bioeffect of interest. Research has also shown the utility of US in addressing the obstacle of the stratum corneum^[33,34] Whilst, provided the delivery challenge can be met, the utility of DNA vaccines in stimulating effective immune responses has also been shown.^[35] However, there are scarce studies into the use of cavitation to impact a co-formulation of DNA plus cavitation agent to achieve transcutaneous delivery, transgene expression, and anti-transgene responses. Indeed, the use of novel stable protein-based cavitation agents opens the possibility that the agent responsible for driving delivery may also possess immune-modulatory properties so that both the delivery technology and the agent it delivers can help to stimulate the desired response. Here we use DNA expressing the model reporter gene luciferase and cavitation nuclei comprised of the model protein BSA to explore this possibility.

Using QPCR and IVIS imaging we demonstrate that delivery via cavitation can achieve up to 30-fold higher number of photons per second per DNA copy delivered than can be achieved by

N+S delivery. This may be a consequence of cavitation offering a route to penetration of the DNA through both plasma and nuclear membranes. Such cavitation-mediated disruption of membranes, as reported and characterized by Liu et al over 2 decades ago,^[36] has recently been elegantly captured by Beekers et al.^[37]

The fact that the resulting anti-luciferase antibody response generated by cavitation-mediated delivery could match or surpass that achieved with needle and syringe is encouraging. Especially in the context of the relatively low amount of DNA actually reaching the dermal compartment, and the “dose-sparing” which may ultimately be possible if cavitation-mediated delivery can be further optimized. Specifically, the area of skin exposed could be increased by adaptation of the focal region of the current transducer using absorber rings, or with clinical translation and adaptation to human skin in mind, an array of transducers covering a wider exposure area could be deployed.

The pCaN formulation methodology described here takes a different route to produce particles of similar morphology and cavitation nucleation activity to the polymeric “nanocups” described by Kwan et al,^[38] which have recently entered clinical trials (IS-RCTN Number 17598292). However, the major distinction, that these pCaN are comprised of protein, adds an extra layer of utility. Specifically, the cavitation agent responsible for the delivery of the therapeutic is no longer inert but can be selected to induce or enhance vaccine responses. This was demonstrated here with the use of pCaN comprised of the model protein bovine serum

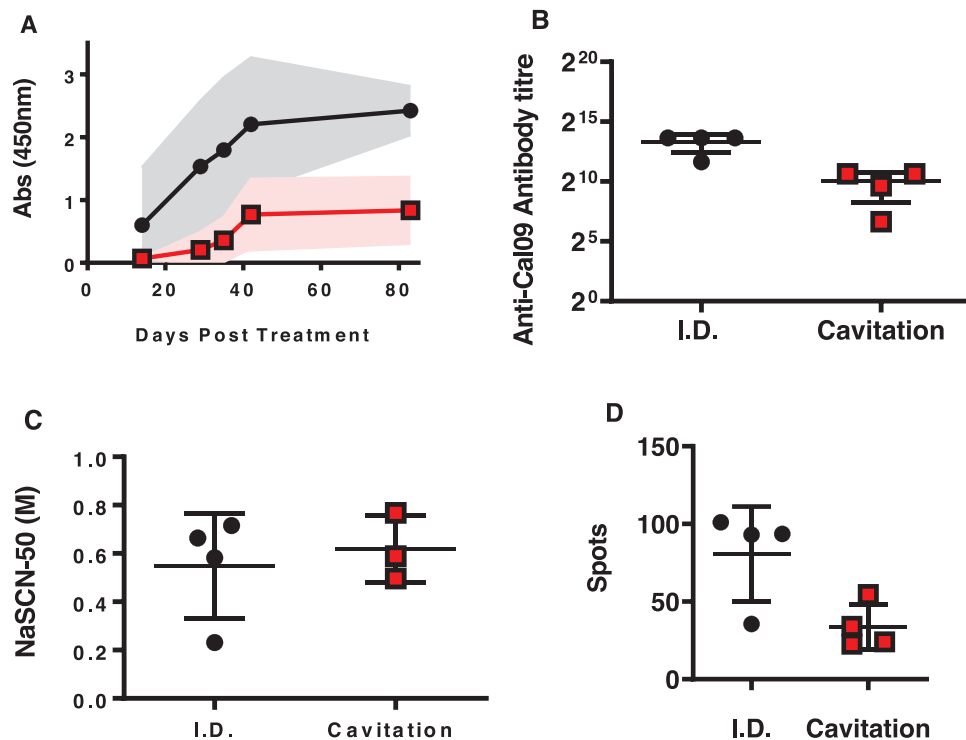


Figure 6. Immune responses to Cal09 protein following delivery of Cal09 plasmid, using cavitation-mediated pCaN nucleated delivery or intradermal injection with N+S. Panel A shows the output of anti-Cal09 ELISA performed on bleeds taken at time points up to 83 days post-prime, (boosting was performed on day 21). Samples tested at a 1:200 dilution, data point represents the mean of values from 4 mice, the shaded area shows standard deviation. Panel B shows titring of anti-Cal09 antibodies by dilution of day 83 serum samples. Panel C represents antibody affinity as a function of the concentration of sodium thiocyanate which halves the Abs 450 nm value (NaSCN-50), a 1 in 200 dilutions was used. Panel D shows ELISpot data from an analysis performed on spleens rescued from mice culled at day 83.

albumin, which not only nucleated cavitation to propel DNA plasmids into the skin but also generated robust and rapid (within 7 days) anti-BSA antibody responses. This is in accordance with the self-propelling activity and dermal deposition of nanocups, as reported in.^[13] In separate work (data not shown) we have demonstrated that pCaN can be generated from a wide range of proteins, raising the possibility of future studies carefully selecting the pCaN protein so that it matches the vaccine or adjuvant effect required. To date, there are no other reports of immunomodulatory proteins being used to formulate cavitation nuclei. It was hoped the data obtained with luciferase plasmid and BSA pCaN would be replicated when luciferase plasmid was replaced with a plasmid expressing the flu antigen “Cal09”. Whilst robust and long-lasting anti-Cal09 HA responses were generated following cavitation-mediated delivery (2 doses 21 days apart), the levels were substantially lower than those produced using needle and syringe (Figure 6A,B). Although, the antibodies demonstrated high affinity and a cellular response was also raised it is clear that further enhancements to the cavitation-mediated delivery are required. The discrepancy between anti-luciferase and anti-Cal09 responses may relate to differing half-life, processing, or MHC presentation levels and timelines of the two proteins. Further, future investigation of this point is needed to untangle these aspects from the potential immune stimulation provided by cavitation per se.

Future enhancements to this proof-of-concept system may be in the form of an improved US set-up designed to increase the

area of skin exposed, modifications to the solvent used to suspend the plasmid and pCaN^[39] or the use of antigens such as SARS-CoV-2 spike protein or cytokine proteins or peptides (e.g., interleukin-1^[40]) to form the pCaN rather than BSA. A study of the impact of the pCaN formulation process on the structure and function of such proteins and peptides will be an essential step in developing this approach. In addition, a deeper understanding of the impact of US parameters on the cell types and immune system within the dermal layers, such as developed by,^[32] will also be of use in progressing the work. Indeed, with regard to the mechanisms underlying the process of sonophoresis, it has been long established that both cavitation and thermal effects contribute to transcutaneous delivery.^[25] The capability we have to monitor cavitation and the link we show between levels of cavitation and levels of delivery will continue to be of use in progressing this mechanistic understanding.

4. Experimental Section

Formation of Cavitation Nuclei: Bovine Serum Albumin (BSA, Sigma Aldrich, ≥99% purity) was added to ultrapure water (Milli-Q) at a concentration of 50 mg mL⁻¹. After vortexing and passing through a 0.22 μm filter, the BSA solution was then aliquoted into glass vials. To each glass vial, ≥99% hexane (32293, Sigma-Aldrich, UK) was added in a 3:1 volume ratio of BSA to hexane. The solution was then sonicated using a probe sonicator (Q125, Q-Sonic, USA) for 3 min at 50% amplitude. The sample was transferred into a large round-bottomed flask, which was then attached

to a rotary evaporator (B205, BUCCHI, USA). The flask was then reduced to dryness over hours, during which the pressure was lowered gradually to a minimum of 30 mbar. After drying, an appropriate volume of Milli-Q was added to restore a BSA concentration of 50 mg mL⁻¹, and the resulting suspension was aliquoted into lyophilization flasks fitted with vented rubber caps.

These flasks were snap-frozen in liquid nitrogen and then placed into a freeze-drying machine (VirTis Advantage Plus 100024341, SP Industries, Inc.). This was sealed and the chamber evacuated, with the vials held at vacuum at <4 Torr for a minimum of 48 h, at a controlled shelf temperature of -20°C. After drying, the vials were removed, and Milli-Q was added in the appropriate volume to reproduce a BSA concentration of 50 mg mL⁻¹. The resultant sample was then used for all further studies. The process of formulation is represented in schematic Figure S5 (Supporting Information).

DLS Analysis, Electron Microscopy, and Videodrop Analysis: Particle size was analysed by differential light scattering, performed on a Malvern Zetasizer Nano ZS (ZEN3600). Measurements were performed on samples diluted 1:100 with 10 mM HEPES/10 mM NaCl buffer pH 7.4, resulting in a protein concentration of 0.5 mg mL⁻¹. All size measurements were conducted using disposable 2 mL Malvern cuvettes. Pre-loaded values for protein light absorbance were used when running measurements, and high-resolution scans were used when possible. Data represents mean values taken from 3 separately prepared samples analyzed 3 times for a minimum of 10 sub-runs.

For Electron Microscopy a ten-fold dilution of a typical pCaN formulation was made using MilliQ water and 20 µL of this was applied to a carbon film-coated 300 mesh copper grids (Electron Microscopy Sciences, Hatfield, PA, USA), which had been pre-ionized in a plasma cleaner for 30 s. After 30 s of application, the grid was blotted dry using filter paper and then negatively stained by incubation with a 10 µL drop of 2% w/v uranyl acetate for 30 s. Excess uranyl acetate was then removed via a blotting with fresh filter paper and samples were then visualized at 80 kV with an FEI Tecnai T12 electron microscope.

For Videodrop (Myriade, Paris, France) analysis, several dilutions of stock sample in 10 mM HEPES pH7.4, 10 mM NaCl were tested to achieve concentrations within the measurable range in accordance with the manufacturer's instructions. All measurements were performed on 3 independently prepared samples.

Zeta Potential: Surface charge measurements were conducted using a Malvern Zetasizer Nano ZS (ZEN3600) and a reusable folded capillary cell (DTS 1070). Samples were diluted in 10 mM HEPES pH7.4, and 10 mM NaCl. Data represents mean values taken from three separately prepared samples analyzed three times for a minimum of ten sub-runs.

In vitro and in vivo Ultrasound Exposure and Cavitation Characterisation: In vitro studies were performed with the set-up as in Figure S1B (Supporting Information). For in vivo studies (Figure S1C) female BALB/c mice were obtained from Charles River Laboratories (USA) by the Biomedical Services at the John Radcliffe Hospital (Oxford, United Kingdom). All mice were kept in groups of up to 12, in individually ventilated cages, under standardized and controlled living environments, under a Home Office approved project license in line with Home Office Legislation and Oxford University Gold Standard (project licence PCB113E8E). All procedures were performed by appropriately trained Home Office personal license holders.

On the day of treatment, female BALB/c mice were anesthetized with 2% isoflurane and 98% oxygen at 2 L mi⁻¹n flow rate. The treatment site was shaved with an electric razor. A depilatory cream (VEET, Reckitt, UK) was applied to ensure full removal of the hair and rinsed off after 1 min. Intradermal delivery was used as a positive control in experiments because although studies directly comparing matched doses of naked DNA delivered via intradermal or intramuscular injection were scarce, Lodmell et al have demonstrated a substantial advantage for intradermal versus intramuscular N+S injection.^[41]

The US parameters are represented in Figure S1D (Supporting Information). Parameters were based on previous studies that had demonstrated safety and efficacy for the delivery of proteins into the skin.^[13] A signal was generated by a waveform generator (33250A, Agilent, United King-

dom), using the parameter set (Frequency 265 kHz, Duty cycle 10%, Pulse repetition frequency 10 Hz, pulse length 10 ms). This was passed to a high-power radiofrequency (RF) amplifier (E&I 1040L RF Amplifier, Electronics & Innovation, Ltd, USA). A matching network (H-117 SIN-001, Sonic Concepts, USA) was used to match the impedance of the output of the amplifier to the transducer. The transducer (117D-01, Sonic Concepts, USA) was fitted with a Perspex coupling cone, filled with degassed water, and covered with an acoustically transparent Mylar membrane. The coupling cone was designed to align with the outer envelope of the focused US beam. The calibration of the acoustic field is described in Figure S6 (Supporting Information). A treatment bed including a formulation holder, containing the DNA and pCaN solution, was placed on the transducer. To allow the cavitation signal to be recorded, a passive acoustic detector (PCD) was coaxially located inside the driving transducer. The PCD signal was passed through a pulse-receiver (DPR300 ultrasonic pulser/receiver, JSR Ultrasonics, Pittsford, NY, USA) set to 23 dB relative gain and a 1.8 MHz high pass filter and 50 Ohm resistance. The signal was then digitized at 25 MHz by an 8-bit digital oscilloscope (Handyscope HS3 100 MHz, TiePie Engineering, The Netherlands) before the data was saved on an external hard drive (Portable SSD T5, Samsung, Korea). Due to limitations in data transfer speeds and data storage requirements, cavitation detected by the PCD could only be recorded for 4 out of the 10 ms of each US pulse, but it was ensured that the full signal was adequately represented by this sub-sample.

For spectrum processing, the data from each US pulse was resampled to 25.175 MHz – an integer multiple of the fundamental system drive frequency of 265 kHz – to enable the separation of the inertial and non-inertial components. A Tukey window was then applied to smoothly terminate the signal before conversion to the Fourier domain and a spectrogram was generated for each treatment, showing frequency (MHz) and energy spectral density (dB re nJ/Hz) on γ_1 and γ_2 axes and time (seconds) on the x-axis.

Separately, the total acoustic sensor energy (TASE) was calculated with the following formula:

$$TASE = \sum_n^{i=n} \frac{(V_{rms}(i))^2}{Z} * T_{pulse} * R_{recorded} \quad (1)$$

where $V_{rms}(i)$ is the root mean square of the i^{th} windowed signal, Z is the impedance of the PCD (50 Ω), T_{pulse} is the length of the drive signal (10 ms), and $R_{recorded}$ is the ratio of the number of actual and recorded pulses.

Before treatment, the pulse receiver was used to assess the beam path for the presence of macrobubbles. To assess disruptions, the set-up was used in transmit mode, and for delivery of treatments the set-up was used in RCV mode.

For the transdermal delivery, approximately 1.8 mL of the formulation was placed in the formulation holder. The mice were placed on top of the US set-up and the scruff was secured with an US gel-coupled acoustic absorber on top of the formulation holder.

After exposure, the excess formulation was removed by rinsing the treatment area with water and drying the skin with clean tissue. The treated area was encircled with a permanent marker pen and delivery or expression was measured by QPCR or IVIS.

Preparation of DNA Plasmids: pGL4.50[luc2/CMV/Hygro] Vector (#E1310, Promega, USA) (CMV-Luc) was purchased and transformed into NEB® Turbo Competent *E. coli* cells (C2984H, NEB). The plasmid proTLx-K B5x4 Cal09 HA, encoding the haemagglutinin from the influenza strain H1N1 A/California/07/2009 (Cal-09), was kindly donated by Touchlight Genetics. The plasmid CMV-Perforin, included to provide an adjuvant effect,^[42] was created by inserting the murine perforin gene, derived from GenBank accession number XM_006513370 [248-1873] into the backbone of proTLx-K B5x4 (Touchlight Ltd, UK). An *E. coli* strain for each of these plasmids was generated to enable in-house production of plasmids for treatment.

These strains were generated by transforming competent cells according to the manufacturer's instruction for 5-alpha Competent *E. coli* (High Efficiency) (NEB). In short, the competent cells were thawed for 10 min

on ice. 1 pg–100 ng of plasmid DNA was added to the cell mixture, flicking to mix, and the mixture was kept on ice for 30 min. The cells were heat shocked at 42°C for 30 s and placed on ice for 5 min. 950 µL of SOC medium (2% Vegetable Peptone, 0.5% Yeast Extract, 10 mM NaCl, 2.5 mM KCl, 10 mM MgCl₂, 10 mM MgSO₄, 20 mM Glucose) (NEB) was added. The cells were placed at 37 °C for 1 h. Dilutions were plated on appropriate LB-agar plates. Glycerol stocks were prepared for all completed DNA constructs. A 40% glycerol in MilliQ stock solution was made and sterilized with a 0.2 µm filter (Thermo Scientific Nalgene, USA). An overnight bacterial culture was mixed 1:1 with the glycerol stock and placed on ice for 10 min. The solutions were subsequently stored in a –80 °C freezer.

Overnight cultures were grown in 5 mL of sterile liquid LB broth (Luria low salt) (L3397, Sigma) or LB Broth, Vegitone (28713, Sigma) with 100 µg mL⁻¹ ampicillin (Sigma) from frozen glycerol stocks. For large-scale purification of DNA, a starter culture was diluted 1:100 in 1L of broth with a selection marker. This was grown in 3×1L Erlenmeyers. Cells were cultured at 37 °C at 220 rpm overnight in a SI-300R shaking incubator (Medline Scientific).

Cell broth was spun down in a 5804R centrifuge (Eppendorf, UK) in 250 mL bottles. The supernatant was disposed of, and the cell pellet was used for subsequent purification. The cell pellets were stored at –80 °C until used. Plasmid DNA was isolated from 1 L of cell broth with the GenElute HP Endotoxin-Free Plasmid Megaprep Kit (Sigma) or from 2 L of cell broth with the GenElute HP Endotoxin-Free Plasmid Gigaprep Kit (Sigma), according to manufacturer's instructions for maximal final concentration.

IVIS Imaging: The mice were imaged after 24 h with an In Vivo Imaging System (IVIS, PerkinElmer, USA). They were anaesthetized with 2% isoflurane and 98% oxygen at 2 L mi⁻¹n flow rate. 100 µL of 15.8 mg mL⁻¹ Pierce D-luciferin (88294, ThermoFisher Scientific, USA) was injected into the tail vein. The mice were imaged 3.5 min after injection and imaged for 30 s. The images were processed with Living Image® (PerkinElmer®, USA). The treatment area was digitally selected and the luminescence (photons per sec) was determined. The luciferase signal was displayed with bioluminescence intensity color bars, scaled to cover the full range of intensity.

qPCR for Quantification of Delivery and Retention in Skin: The gross level of DNA delivered to the whole skin sample was measured. Skin tissue was cut into small pieces and 1x Promega Lysis Buffer (E1531, Promega, USA) was added to a final dilution of 125 mg skin per 1 mL of buffer. This was frozen at –80 °C and then thawed. The thawed suspension was placed in a GentleMacs C tube (130-093-237, Miltenyi Biotec, Germany) and homogenized with a GentleMacs dissociator (Miltenyi Biotec, Germany) by running the predefined Multi_H_01 program five times. This solution was spun down at 800xg for 1 min. 200 µL of the homogenized supernatant was sampled and used for DNA extraction and quantification. The skin was subsequently processed with the GenElute Mammalian Genomic DNA Miniprep Kit (Sigma-Aldrich). In short, the 20 µL RNase was added and the cells were lysed with 200 µL of Lysis Solution C and 20 µL proteinase K solution (20 mg mL⁻¹). This was vortexed for 15 s and incubated at 70 °C for 10 min. All subsequent steps, column preparation, binding, washing, and elution, were done exactly according to the manufacturer's instructions. 5 µL of this elution was used for qPCR quantification. If the qPCR values were not within the standard curve, the elution was diluted 10000-fold and 5 µL of the dilution was used.

A mastermix containing the primers (CTTCGAGGAGGACTATTCTTG, GTCGTA CTGCTGATGAGAGTG), probe ([6FAM]TGCTGGTCCACACATATTAGCT[TAMRA]), 2x qPCR BIO Probe Mix Hi-ROX (PB20.22-01, PCR Biosystems Ltd., UK) and nucleotide-free water was prepared, according to manufacturer's instructions. 5 µL of eluted DNA, which was either from a sample or a spiked control, was added to 15 µL of the mastermix. The solution contained a final concentration of 400 nM of forward and reverse primers, 200 nM of the TAM-FAMRA labeled probe, polymerase, nucleotides, buffers, and ROX dye as a reference.

Standard curves were prepared by spiking untreated skin with a known number of CMV-Luc DNA copies. The skin was then processed in an identical way to the samples as described above.

The plate was analyzed on a StepOnePlus Real-Time PCR System (Applied Biosciences). The cycling conditions for the qPCR were 95 °C for

2 min for DNA denaturing and 40 cycles of 95 °C for 5 s and 60 °C for 30 s.

ELISA for Anti-Luciferase Antibodies, anti-BSA Antibodies, and anti-Cal09 Antibodies: Antibody response to luciferase protein, Cal09 HA protein, and BSA protein was quantified using standard ELISA procedures as follows. Firstly, a Maxisorp 96-well plate (DIS-971-010P (439454), Nunc ImmunoPlates) was coated with either 50 µL per well of recombinant firefly luciferase protein (ab100961, AbCam, UK) for the anti-luciferase ELISA, or with 50 µL per well of 99% purity BSA (A7638, Sigma Aldrich, UK) or a 10 µg mL⁻¹ Cal09 protein (IT-003-SW12p, Immune Technology Corp., USA). The plate was then sealed with ELISA sealing film (LW2771, Alpha Laboratories), and was left overnight at 4 °C for protein adhesion. The next day, the seal was removed, and the plate was emptied and washed six times with 0.05% Tween20 detergent in PBS. After washing, the plates were smacked firmly on padded tissue paper until any visible droplets in the wells were removed. This washing process was repeated throughout various stages of the ELISA and future references will truncate this explanation to a "washing step".

Once dry, 50 µL of Pierce Protein-Free (PBS) Blocking Buffer (37572, ThermoFisher Scientific, USA) was pipetted into each well. A new seal was applied to the plate, and incubation for 1 h at RT was performed. During this time, the samples were prepared by diluting pre-drawn samples of mouse tail-bleed serum to 100x in PBS. A calibration curve was also made up using a serial dilution of Firefly Luciferase Monoclonal antibody, produced in mouse (MA1-80225, ThermoFisher Scientific, USA) for anti-luciferase assays, or Anti-Bovine Serum Albumin antibody, produced in rabbit (ab186531, AbCam, UK) for anti-BSA assays. The washing step was repeated, and the samples were placed on the plate in duplicate, following which the plate was again sealed and left to incubate at RT for 2 h.

Before completion of the incubation period, a 1:10 000 dilution of secondary antibody was made, using either anti-mouse goat IgG HRP for anti-luciferase assays (31430, ThermoFisher Scientific, USA) or anti-rabbit goat IgG HRP for anti-BSA assays or anti-Cal09 assays (31466, ThermoFisher Scientific, USA). After incubation and the washing step, before adding the secondary antibody, sodium thiocyanate (1066272500, Merck Millipore, USA) was added in increasing concentrations and the plate was washed after 10 min when avidity was assessed. Then the plate was coated with 50 µL per well of the requisite secondary antibody, sealed, and incubated for 1 h at room temperature. Following this step, the washing step was repeated, and 50 µL of Ultra-TMB HRP substrate (PN34028, ThermoFisher Scientific, USA) was added to each well. The plates were sealed and protected from light while the assay developed. After 10–30 min, the reaction was stopped with 50 µL of stop solution (0.5 M H₂SO₄) per well. The plate was then placed in a plate reader (BMGLabTech, FLUOstar Omega, Germany), and the absorbance data at 450 nm was used for calculations of protein concentrations in the blood samples, by cross-referencing with the calibration curve produced.

ELISpot Analysis: To determine the interferon-γ secretion by splenocytes upon stimulation with haemagglutinin Cal09, the mouse IFN-γ ELISpot PLUS (HRP) (3321-4HST-2, Mabtech, Sweden) kit was used to perform an ELISpot.

15 mL falcon tubes with 5 mL RPMI-1640 Medium (ThermoFisher Scientific, USA) with 10% Fetal Bovine Serum (qualified, Brazil) (10270106, ThermoFisher Scientific, USA) were prepared. For collecting the spleen, a mouse was culled, its fur wetted with 70% ethanol, and the body cavity was cut open and the spleen removed. The spleen was placed straight into the prepared falcon tubes with the RPMI-1640+10% FBS at room temperature.

In a tissue culture hood, a 70 µm cell strainer (10788201, Thermo Fisher Scientific) was prewetted with 1 mL RPMI-1640+10% FBS media. The plunger end of a 3 mL syringe was used to mash the spleen through the cell strainer into a 55–60 mm petri dish to get a single cell suspension. Afterward, the cell strainer was rinsed with 5 mL RPMI-1640+10% FBS to remove any remaining splenocytes.

The ELISpot plate with the required number of strips was assembled and washed four times with sterile PBS. This was conditioned with 200 µL of RPMI-1640+10% FBS per well whilst the splenocytes were processed.

The cell suspension was transferred from the petri dishes to 15 mL falcon tubes and spun down for 3 min at 800xg. The supernatant was then discarded and the pellet was resuspended in 1 mL Red Blood Cell Lysis buffer (11814389001, Sigma). This was incubated for 5–10 min. 9 mL of RPMI-1640+10% FBS was added to this and the suspension spun down again at 800xg for 3 min. The supernatant was discarded and the cells were resuspended in 3 mL RPMI-1640+10% FBS. A 4 µL cell suspension aliquot was dissolved 1:5 in RPMI-1640+10% FBS and mixed 1:1 with trypan blue solution, 0.4% (15250061, ThermoFisher Scientific). The cells were counted using a hemocytometer.

The positive control concanavalin A from *Canavalia ensiformis* (Jack bean) (L7647-25MG, Sigma) was dissolved to 1 µg µL⁻¹, the same concentration as the haemagglutinin Cal09 protein stock. Both the haemagglutinin Cal09 protein and the concanavalin A stocks were dissolved 1:10 in RPMI-1640+10% FBS.

The media was removed from the ELISpot plate and for every splenocyte sample, 50 µL of media was added to two wells, 50 µL of haemagglutinin dilution was added to two wells, and 50 µL of concanavalin A dilution was added to two wells. 100 000 splenocytes were then carefully added to each of these six wells per splenocyte sample to a total volume of 100 µL.

The plate was incubated for 21.5 h at 37 °C in a humidified incubator with 5% CO₂, wrapped in cling film or aluminum foil to prevent evaporation. The following day, the cells were removed and the plate was washed five times with 200 µL PBS per well. The interferon-γ detection antibody (R4-6A2-biotin), which was part of the mouse IFN-gamma ELISpot PLUS (HRP) kit, was dissolved in 1 µg mL⁻¹ in PBS containing 0.5% fetal bovine serum (10270106, ThermoFisher Scientific, USA). 100 µL detection antibody was added to each well and incubated at room temperature for 2 h. The plate was then washed five times with 200 µL PBS per well. The streptavidin-HRP, also part of the kit, was dissolved 1:1000 in PBS containing 0.5% fetal bovine serum. A 100 µL per well of the streptavidin-HRP was added to each well and incubated at room temperature for 1 h. The plate was again washed five times with 200 µL PBS per well. Then 100 µL per well of the supplied TMB substrate solution was added and the plate was left to develop until distinct spots emerged. The color development was stopped by extensive washing with deionized water, including the undersides of the membrane. The plate and strips were left to dry overnight and then reassembled. The plate was imaged using AID ELISpot reader and software (AID Diagnostika GmbH, Germany).

The total number of spot-forming units was calculated by subtracting the spots in the negative wells. The spots were then corrected to spot-forming units per 10⁶ cells.

Sectioning and Staining of Skin Tissue: Mice were culled 24 h after treatment and the treated skin was harvested. The skin was placed in a 10% formalin solution, neutral buffered (HT501128, Sigma) for fixing, and transferred to 70% ethanol after 24 h. After dehydration and penetration by paraffin overnight, using an Excelsior AS (Thermo Scientific) sample was embedded in a paraffin block. Sections of 4 µm were cut with an HM 355 S rotary microtome (Eprelia, USA). Slices were floated and attached to microscope slides. After cooling for 2 days staining with hematoxylin and eosin was performed using standard procedures and hematoxylin (Hematoxylin Solution, Harris Modified, HHS-16, Merck) and eosin stain (1 g Eosin Y disodium salt, E-6003, Sigma in 100 mL 70% ethanol). Any excess eosin was removed by rinsing the slides in tap water. To dehydrate the samples, the slides were submerged in 70% ethanol for 30 s, 90% ethanol for 30 s, in absolute ethanol for 1 min, a second time in absolute ethanol for 2 min, histoclear for 5 min, and a second time in histoclear for 5 min. The slides were then mounted using VectaMount Mounting Medium (H-5000).

Supporting Information

Supporting Information is available from the Wiley Online Library or from the author.

Acknowledgements

J.H. was supported by the EPSRC CDT in Synthetic Biology EP/L016494/1, and J.B. by the All Souls College Hugh Springer Graduate Fellowship. All authors were grateful for the generous benefaction of Mr Donald Porteous who supported all experimental aspects of this work and the EPSRC under the Oxford Centre for Drug Delivery Devices grant EP/L024012/1.

Conflict of Interest

The authors declare no conflict of interest.

Data Availability Statement

The data that support the findings of this study are openly available in Oxford University Research Archive at <https://ora.ox.ac.uk/>, reference number [1].

Keywords

cavitation nuclei, delivery, DNA, nano, transcutaneous, ultrasound, vaccines

Received: July 5, 2023

Revised: August 21, 2023

Published online: September 1, 2023

- [1] WHO, **2023**. <https://www.who.int/news-room/fact-sheets/detail/immunization-coverage> (accessed: September 2023).
- [2] A. M. Hauri, G. L. Armstrong, Y. J. Hutin, *Int J STD AIDS* **2004**, *15*, 7.
- [3] N. T. Weissmueller, H. A. Schiffter, A. J. Pollard, *Expert Rev. Vaccines* **2013**, *12*, 687.
- [4] J. Pepin, C. N. Abou Chakra, E. Pepin, V. Nault, *PLoS One* **2013**, *8*, e80948.
- [5] C. E. Cooke, J. M. Stephens, *Med Devices (Auckl)* **2017**, *10*, 225.
- [6] J. P. Amorij, W. Hinrichs, H. W. Frijlink, J. C. Wilschut, A. Huckriede, *Lancet Infect. Dis.* **2010**, *10*, 699.
- [7] N. T. Weissmueller, H. A. Schiffter, R. C. Carlisle, C. S. Rollier, A. J. Pollard, *Clin. Vaccine Immunol.* **2015**, *22*, 586.
- [8] K. Schulze, T. Ebensen, P. Riese, B. Prochnow, C. M. Lehr, C. A. Guzman, *Curr. Top. Microbiol. Immunol.* **2016**, *398*, 207.
- [9] J. Hetta, R. Carlisle, *Vaccines (Basel)* **2020**, *8*, 534.
- [10] R. Carlisle, J. Choi, M. Bazan-Peregrino, R. Laga, V. Subr, L. Kostka, K. Ulbrich, C. C. Coussios, L. W. Seymour, *J Natl Cancer Inst* **2013**, *105*, 1701.
- [11] R. Myers, C. Coviello, P. Erbs, J. Follope, C. Rowe, J. Kwan, C. Crake, S. Finn, E. Jackson, J. M. Balloul, C. Story, C. Coussios, R. Carlisle, *Mol. Ther.* **2016**, *24*, 1627.
- [12] M. Grundy, L. Bau, C. Hill, C. Paverd, C. Mannaris, J. Kwan, C. Crake, C. Coviello, C. Coussios, R. Carlisle, *Nanomedicine (Lond)* **2021**, *16*, 37.
- [13] S. Bhatnagar, J. J. Kwan, A. R. Shah, C. C. Coussios, R. C. Carlisle, *J Control Release* **2016**, *238*, 22.
- [14] C. Levin, H. Perrin, B. Combadiere, *Hum Vaccin Immunother* **2015**, *11*, 27.
- [15] R. T. Kenney, S. A. Frech, L. R. Muenz, C. P. Villar, G. M. Glenn, *N. Engl. J. Med.* **2004**, *351*, 2295.
- [16] M. A. Liu, *Immunol Rev* **2011**, *239*, 62.
- [17] A. A. Walters, E. Kinnear, R. J. Shattock, J. U. McDonald, L. J. Caproni, N. Porter, J. S. Tregoning, *Gene Ther.* **2014**, *21*, 645.

- [18] H. Zhang, K. Rombouts, L. Raes, R. Xiong, S. C. De Smedt, K. Braeckmans, K. Remaut, *Adv. Biosyst.* **2020**, *4*, 2000057.
- [19] S. Hirobe, H. Azukizawa, T. Hanafusa, K. Matsuo, Y. S. Quan, F. Kamiyama, I. Katayama, N. Okada, S. Nakagawa, *Biomaterials* **2015**, *57*, 50.
- [20] J. H. Jung, S. G. Jin, *J Pharm Investig* **2021**, *51*, 503.
- [21] D. Xia, R. Jin, G. Byagathvalli, H. Yu, L. Ye, C. Y. Lu, M. S. Bhambha, C. Yang, M. R. Prausnitz, *Proc Natl Acad Sci U S A* **2021**, *118*, e2110817118.
- [22] A. Patel, J. N. Walters, E. L. Reuschel, K. Schultheis, E. Parzych, E. N. Gary, I. Maricic, M. Purwar, Z. Eblimit, S. N. Walker, D. Guimet, P. Bhojnagarwala, O. S. Adeniji, A. Doan, Z. Xu, D. Elwood, S. M. Reeder, L. Pessaint, K. Y. Kim, A. Cook, N. Chokkalingam, B. Finneyfrock, E. Tello-Ruiz, A. Dodson, J. Choi, A. Generotti, J. Harrison, N. J. Tursi, V. M. Andrade, Y. Dia, et al., *Cell Rep Med* **2021**, *2*, 100420.
- [23] J. J. Choi, R. C. Carlisle, C. Coviello, L. Seymour, C. C. Coussios, *Phys Med Biol* **2014**, *59*, 4861.
- [24] A. Tezel, S. Paliwal, Z. Shen, S. Mitragotri, *Vaccine* **2005**, *23*, 3800.
- [25] D. Park, H. Park, J. Seo, S. Lee, *Ultrasonics* **2014**, *54*, 56.
- [26] E. Stride, C. Coussios, *Nat. Rev. Phys.* **2019**, *1*, 495.
- [27] Y. Hu, J. M. Wan, A. C. Yu, *Ultrasound Med Biol* **2013**, *39*, 2393.
- [28] M. Dupuis, K. Denis-Mize, C. Woo, C. Goldbeck, M. J. Selby, M. Chen, G. R. Otten, J. B. Ulmer, J. J. Donnelly, G. Ott, D. M. McDonald, *J. Immunol.* **2000**, *165*, 2850.
- [29] U. R. Hengge, B. Dextling, A. Mirmohammadsadegh, *J. Invest. Dermatol.* **2001**, *116*, 979.
- [30] D. Sawamura, K. Yasukawa, K. Kodama, K. Yokota, K. C. Sato-Matsumura, T. Toshihiro, H. Shimizu, *J. Invest. Dermatol.* **2002**, *118*, 967.
- [31] R. Myers, M. Grundy, C. Rowe, C. M. Coviello, L. Bau, P. Erbs, J. Foloppe, J. M. Balloul, C. Story, C. C. Coussios, R. Carlisle, *Int J Nanomedicine* **2018**, *13*, 337.
- [32] S. Giantulli, E. Tortorella, F. Brasili, S. Scarpa, B. Cerroni, G. Paradossi, A. Bedini, S. Morrone, I. Silvestri, F. Domenici, *Sci. Rep.* **2021**, *11*, 19033.
- [33] B. C. Seah, B. M. Teo, *Int J Nanomedicine* **2018**, *13*, 7749.
- [34] A. H. Liao, Y. C. Chen, C. Y. Chen, S. C. Chang, H. C. Chuang, D. L. Lin, C. P. Chiang, C. H. Wang, J. K. Wang, *J Control Release* **2022**, *349*, 388.
- [35] P. Tebas, S. Yang, J. D. Boyer, E. L. Reuschel, A. Patel, A. Christensen-Quick, V. M. Andrade, M. P. Morrow, K. Kraynyak, J. Agnes, M. Purwar, A. Sylvester, J. Pawlicki, E. Gillespie, I. Maricic, F. I. Zaidi, K. Y. Kim, Y. Dia, D. Frase, P. Pezzoli, K. Schultheis, T. R. F. Smith, S. J. Ramos, T. McMullan, K. Buttigieg, M. W. Carroll, J. Ervin, M. C. Diehl, E. Blackwood, M. P. Mammen, et al., *EClinicalMedicine* **2021**, *31*, 100689.
- [36] J. Liu, T. N. Lewis, M. R. Prausnitz, *Pharm. Res.* **1998**, *15*, 918.
- [37] I. Beekers, S. A. G. Langeveld, B. Meijlink, A. F. W. van der Steen, N. de Jong, M. D. Verweij, K. Kooiman, *J Control Release* **2022**, *347*, 460.
- [38] J. J. Kwan, S. Graham, R. Myers, R. Carlisle, E. Stride, C. C. Coussios, *Phys Rev E Stat Nonlin Soft Matter Phys* **2015**, *92*, 023019.
- [39] E. E. L. Tanner, A. M. Curreri, J. P. R. Balkaran, N. C. Selig-Wober, A. B. Yang, C. Kendig, M. P. Fluhr, N. Kim, S. Mitragotri, *Adv. Mater.* **2019**, *31*, 1901103.
- [40] A. Tagliabue, D. Boraschi, *Vaccine* **1993**, *11*, 594.
- [41] D. L. Lodmell, M. J. Parnell, J. T. Weyhrich, L. C. Ewalt, *Vaccine* **2003**, *21*, 3998.
- [42] A. C. Shrestha, D. K. Wijesundara, M. G. Masavuli, Z. A. Mekonnen, E. J. Gowans, B. Grubor-Bauk, *Vaccines (Basel)* **2019**, *7*, 38.